AD-A178 805 FULL-WAVE ANALYSIS OF ISOLATED AND COUPLED MICROWAVE TRANSMISSION LINES U... (U) ILLINOIS UNIV AT URBANA ELECTROMAGNETIC COMMUNICATION LAB Z PANTIC ET AL

1/1

UNCLASSIFIED FEB 87 EMC-87-1 ARO-22634 5-EL F/G 9/1 NL

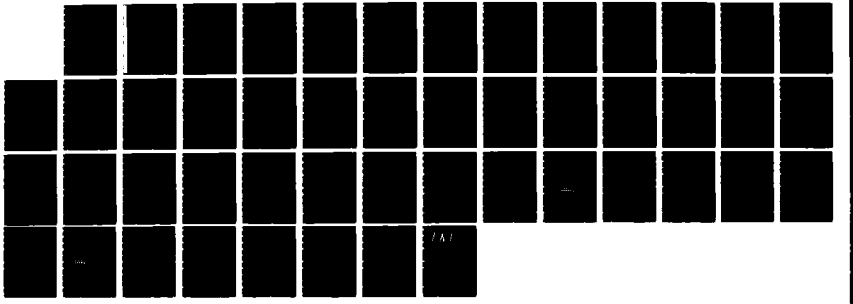

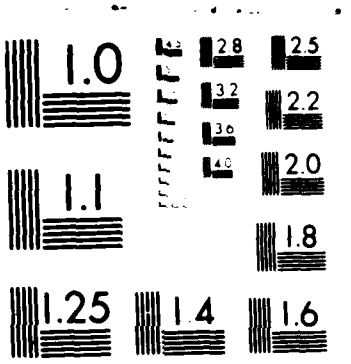

FULL-WAVE ANALYSIS OF ISOLATED AND COUPLED MICROWAVE TRANSMISSION LINES USING THE FINITE ELEMENT METHOD

TECHNICAL REPORT

Z. Pantic
R. Mittra

February 1987

SUPPORTED BY

U. S. ARMY RESEARCH OFFICE

GRANT NO. DAAG 29-85-K-0183

ELECTROMAGNETIC COMMUNICATION LABORATORY
DEPARTMENT OF ELECTRICAL AND COMPUTER ENGINEERING
UNIVERSITY OF ILLINOIS
URBANA, IL 61801

APPROVED FOR PUBLIC RELEASE.
DISTRIBUTION UNLIMITED.

THE FINDINGS IN THIS REPORT ARE NOT TO BE CONSTRUED AS AN OFFICIAL DEPARTMENT OF THE ARMY POSITION, UNLESS SO DESIGNATED BY OTHER AUTHORIZED DOCUMENTS.

UNCLASSIFIED
SECURITY CLASSIFICATION OF THIS PAGE

REPORT DOCUMENTATION PAGE

1a REPORT SECURITY CLASSIFICATION Unclassified	1b. RESTRICTIVE MARKINGS
2a. SECURITY CLASSIFICATION AUTHORITY	3. DISTRIBUTION / AVAILABILITY OF REPORT Approved for public release; distribution unlimited.
2b. DECLASSIFICATION / DOWNGRADING SCHEDULE	
4. PERFORMING ORGANIZATION REPORT NUMBER(S) EMC 87-1; UILU-ENG-87-2542	5. MONITORING ORGANIZATION REPORT NUMBER(S) ARO 22634.5-EL
6a. NAME OF PERFORMING ORGANIZATION Electromagnetic Communication Laboratory 6b OFFICE SYMBOL (If applicable)	7a. NAME OF MONITORING ORGANIZATION U. S. Army Research Office
6c. ADDRESS (City, State, and ZIP Code) Department of Elec. and Computer Engineering University of Illinois Urbana, Illinois 61801	7b. ADDRESS (City, State, and ZIP Code) P. O. Box 12211 Research Triangle Park, NC 27709-2211
8a. NAME OF FUNDING / SPONSORING ORGANIZATION U. S. Army Research Office 8b. OFFICE SYMBOL (If applicable)	9. PROCUREMENT INSTRUMENT IDENTIFICATION NUMBER DAAG29-85-K-0183
8c. ADDRESS (City, State, and ZIP Code) P. O. Box 12211 Research Triangle Park, NC 27709-2211	10. SOURCE OF FUNDING NUMBERS PROGRAM ELEMENT NO. / PROJECT NO. / TASK NO. / WORK UNIT ACCESSION NO

11 TITLE (Include Security Classification)
FULL-WAVE ANALYSIS OF ISOLATED AND COUPLED MICROWAVE TRANSMISSION LINES USING THE FINITE ELEMENT METHOD

12 PERSONAL AUTHOR(S)
Zorica Pantic and Raj Mittra

13a. TYPE OF REPORT	13b. TIME COVERED	14. DATE OF REPORT (Year, Month, Day)	15. PAGE COUNT
Technical Report	FROM _____ TO _____	February 1987	45

16. SUPPLEMENTARY NOTATION
The view, opinions and/or findings contained in this report are those of the author(s) and should not be construed as an official Department of the Army position, policy, or decision, unless so designated by other documentation.

17 COSATI CODES		
FIELD	GROUP	SUB-GROUP

18. SUBJECT TERMS (Continue on reverse if necessary and identify by block number)
Microwave Transmission Lines; Finite Element Method; Wave Guides; Full-Wave Analysis

19 ABSTRACT (Continue on reverse if necessary and identify by block number)

This paper describes a finite element approach to a hybrid-mode analysis of isolated and coupled microwave transmission lines. Both the first and higher-order ordinary elements, as well as singular and infinte elements, are used to solve for the eigenvalues and eigenvectors of the modes propagating along the line. Once the field distribution in the cross section of the line is known the characteristic impedance of the dominant mode propagating along the line can readily be obtained. A perturbational approach is developed for estimating the losses due to conductor and dielectric dissipation and computing the attenuation constant for each mode.

Lines treatable by this method may contain an arbitrary number of arbitrarily shaped conductors, including a system of conductors either placed above a single ground plane or between two parallel ground planes, and inhomogeneous dielectric regions that can be approximated locally by a number of homogeneous subregions.

(continued on reverse side)

20 DISTRIBUTION / AVAILABILITY OF ABSTRACT ☐ UNCLASSIFIED/UNLIMITED ☐ SAME AS RPT. ☐ DTIC USERS	21 ABSTRACT SECURITY CLASSIFICATION Unclassified
22a NAME OF RESPONSIBLE INDIVIDUAL	22b. TELEPHONE (Include Area Code) / 22c. OFFICE SYMBOL

DD FORM 1473, 84 MAR — 83 APR edition may be used until exhausted. All other editions are obsolete.

SECURITY CLASSIFICATION OF THIS PAGE
UNCLASSIFIED

19. (cont.)

The results obtained using the finite element procedure have been compared for various types of microwave transmission lines and have been found to agree well with available data.

UILU-ENG-87-2542

Electromagnetic Communication Laboratory Report No. 87-1

FULL-WAVE ANALYSIS OF ISOLATED AND COUPLED MICROWAVE TRANSMISSION LINES USING THE FINITE ELEMENT METHOD

by

Z. Pantic
R. Mittra

Electromagnetic Communication Laboratory
Department of Electrical and Computer Engineering
University of Illinois at Urbana-Champaign
Urbana, Illinois 61801

Technical Report

February 1987

Supported by

U. S. Army Research Office
Grant No. DAAG 29-85-K-0183

TABLE OF CONTENTS

LIST OF FIGURES

ABSTRACT

This paper describes a finite element approach to a hybrid-mode analysis of isolated and coupled microwave transmission lines. Both the first and higher-order ordinary elements, as well as singular and infinite elements, are used to solve for the eigenvalues and eigenvectors of the modes propagating along the line. Once the field distribution in the cross section of the line is known the characteristic impedance of the dominant mode propagating along the line can readily be obtained. A perturbational approach is developed for estimating the losses due to conductor and dielectric dissipation and computing the attenuation constant for each mode.

Lines treatable by this method may contain an arbitrary number of arbitrarily shaped conductors, including a system of conductors either placed above a single ground plane or between two parallel ground planes, and inhomogeneous dielectric regions that can be approximated locally by a number of homogeneous subregions.

The results obtained using the finite element procedure have been compared for various types of microwave transmission lines and have been found to agree well with available data.

I. INTRODUCTION

The accurate prediction of the characteristic impedance, attenuation, coupling, crosstalk, etc., in microstrips, striplines and similar transmission lines is important in microwave and millimeter wave integrated circuits, digital circuit design, communication and other applications. The objective of this paper is to consider microwave transmission lines with rather arbitrary configuration and to present a computer-aided analysis that allows simple and accurate calculation of its design parameters.

In the past, microwave transmission lines have been thoroughly investigated by many authors and many approaches to analyzing them have been devised, e.g., the Green's function techniques [1]-[6], conformal mapping [7]-[9], variational methods [10], [11], Fourier transform method [12], [13], Fourier integral method [14], spectral-domain method [15]-[17], boundary element method [18], [19] and finite element method [20]. All of the above methods, with the exception of the last two, are restricted in their application to transmission lines in which the conductors are thin strips or the dielectric inserts have planar interfaces or both restrictions apply. In contrast, the finite element method (FEM) is capable of handling transmission lines with rather arbitrary configurations, since the lines treatable by this method may contain an arbitrary number of conductors of arbitrary shape and inhomogeneous dielectric regions that can be approximated locally by a number of homogeneous subregions. Because of the generality of the FEM approach the finite element method is employed in this paper for the analysis of several representative microwave transmission lines of practical interest. The analysis is based on a hybrid-mode model which takes into account coupling between TE- and TM-modes propagating along the line.

Both the first- and higher-order ordinary elements, as well as singular and infinite elements, are used in the FEM algorithm to solve for the phase constant (eigenvalues) and the corresponding field distribution (eigenvectors) in a microwave transmission line. The

characteristic impedance of the dominant mode propagating along the line is calculated from the so-called power-current definition [21]-[24]. A perturbation method is used to compute the losses for each mode due to both the conductor and dielectric dissipations.

The characteristic impedance and loss characteristics have been calculated for some transmission lines of interest and very good agreement with available data has been obtained.

II. DESCRIPTION OF THE METHOD

1. Formulation of the Functional

Consider a microwave transmission line with an arbitrary cross section consisting of a number of arbitrarily shaped conductors and inhomogeneous dielectric regions which can be approximated locally by homogeneous subregions (Fig. 1). Let us assume that the line is uniform along the longitudinal (z) axis and let ϵ and μ ($=\mu_0$) denote permittivity and permeability, respectively, of the medium in each homogeneous subregion. The electric and magnetic fields propagating along the line can be written in the following form:

$$\vec{E} = \vec{e}\, e^{-\gamma z} \quad , \quad \vec{H} = \vec{h}\, e^{-\gamma z} \tag{1.1}$$

where $\gamma = j\beta$ is the propagation constant, and β is the phase constant.

After substituting (1) into first and second Maxwell's equation we obtain:

$$\nabla \times \vec{h} - j\beta(\hat{z} \times \vec{h}) = j\omega\epsilon\vec{e} \tag{1.2a}$$

$$\nabla \times \vec{e} - j\beta(\hat{z} \times \vec{e}) = -j\omega\mu\vec{h} \tag{1.2b}$$

where $\omega = 2\pi f$ is the angular frequency of the wave and $\hat{z}$ is the unit vector along z-axis.

Using the reaction concept [25] we derive the mixed-field variational formula for waveguide phase constants. Multiplying equation (1.2a) by $\vec{e}$ and (1.2b) by $\vec{h}$ and

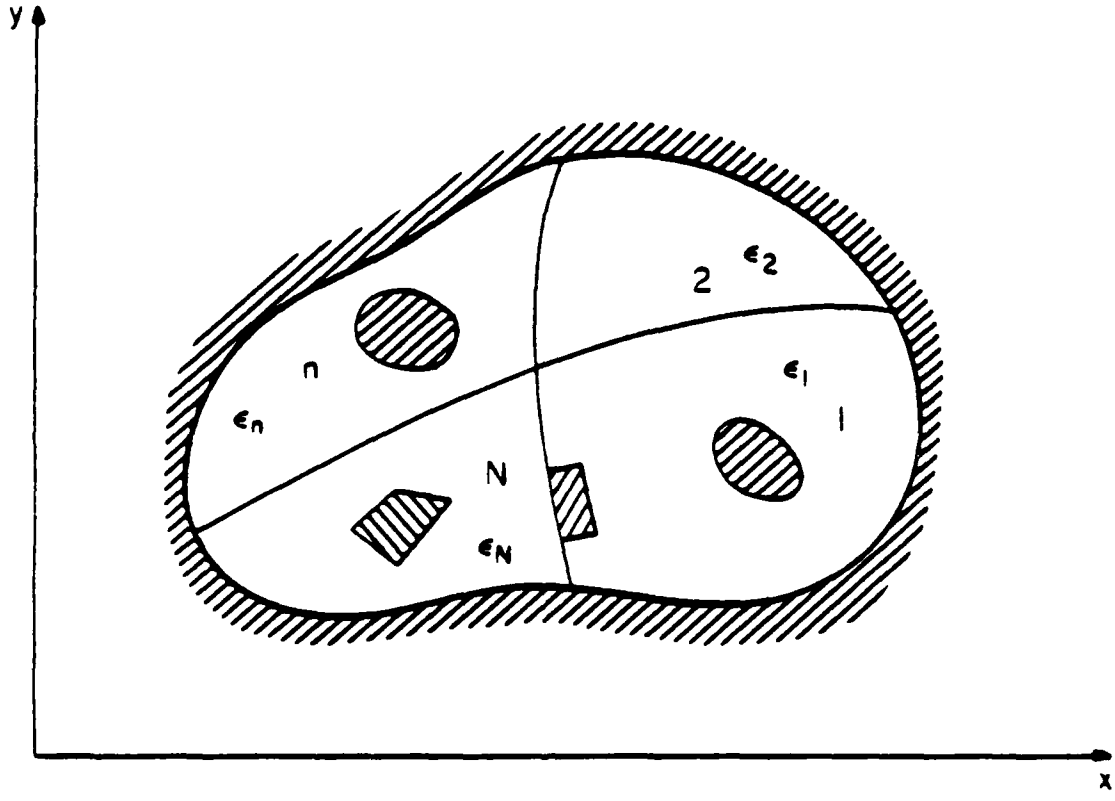

Figure 1. Cross section of a microwave transmission line.

subtracting (1.2b) from (1.2a) we obtain

$$\vec{e}\cdot(\nabla\times\vec{h})-\vec{h}\cdot(\nabla\times\vec{e})-\hat{z}(\vec{h}\times\vec{e})\,j\beta-\hat{z}(\vec{h}\times\vec{e})\cdot j\beta=j\omega(\epsilon e^2+\mu h^2) \quad (1.3)$$

Using the relationship

$$\nabla\cdot(\vec{A}\times\vec{B})=\vec{B}\cdot(\nabla\times\vec{A})-\vec{A}\cdot(\nabla\times\vec{B}) \quad (1.4)$$

and integrating both sides of (1.3) over the cross section, S, the above equation becomes

$$\int_S 2j\beta\hat{z}\cdot(\vec{e}\times\vec{h})ds-\int_S\nabla\cdot(\vec{e}\times\vec{h})ds=j\omega\int_S(\epsilon e^2+\mu h^2)ds \quad (1.5)$$

Finally, after applying Stoke's theorem to (1.5), we obtain

$$\beta=\frac{\omega\int_S(\epsilon e^2+\mu h^2)ds-j\oint_\Gamma(\vec{e}\times\vec{h})\cdot\hat{n}dl}{2\int_S\hat{z}\cdot(\vec{e}\times\vec{h})ds} \quad (1.6)$$

where Γ is the boundary of the cross section S and $\hat{n}$ is the unit normal at the boundary.

Equation (1.6) is the variational formula for β which is stationary for small variations in electromagnetic fields. Reformulated it has the form:

$$\int_S(\epsilon e^2+\mu h^2)ds-\frac{2\beta}{\omega}\int_S\hat{z}\cdot(\vec{e}\times\vec{h})ds-\frac{j}{\omega}\oint_\Gamma(\vec{e}\times\vec{h})\cdot\hat{n}dl=0 \quad (1.7)$$

In the general case electromagnetic fields $\vec{e}$, $\vec{h}$ have both longitudinal (z) and transversal (t) components

$$\vec{e}=\vec{e}_t+e_z\hat{z}$$

$$\vec{h}=\vec{h}_t+h_z\hat{z} \quad (1.8)$$

Transversal fields then can be expressed in terms of longitudinal components e_z, h_z

$$\vec{e}_t=\frac{j\omega\mu}{k^2}\left|(\hat{z}\times\nabla_t h_z)-\frac{\beta}{\omega\mu}\nabla_t e_z\right| \quad (1.9)$$

$$\vec{h}_t = \frac{-j\omega\epsilon}{k^2}\left|(\hat{z}\times\nabla_t e_z) + \frac{\beta}{\omega\epsilon}\nabla_t h_z\right| \tag{1.10}$$

where ∇_t is transversal operator and

$$k^2 = \omega^2\epsilon\mu - \beta^2 \tag{1.11}$$

If we introduce new variables [20]

$$\bar{\beta} = \frac{\beta c}{\omega}\ ,\quad \phi = h_z\ ,\quad \psi = \sqrt{\frac{\epsilon_0}{\mu_0}}\frac{e_z}{\bar{\beta}} \tag{1.12}$$

relations (1.9,10) will become

$$\vec{e}_t = j\sqrt{\frac{\mu_0}{\epsilon_0}}\mu_r\frac{\omega}{c}\frac{1}{k^2}\left|(\hat{z}\times\nabla_t\phi) - \frac{\bar{\beta}^2}{\mu_r}\nabla_t\psi\right| \tag{1.13a}$$

$$\vec{h}_t = -j\bar{\beta}\frac{\omega}{c}\frac{1}{k^2}\left|\nabla_t\phi + \epsilon_r(\hat{z}\times\nabla_t\psi)\right| \tag{1.13b}$$

Using (1.12) and (1.13a, b) we obtain

$$e^2 + \mu h^2 = \mu_0\left\{\mu_r\phi^2 + \bar{\beta}^2\epsilon_r\psi^2 - \left(\frac{\omega}{c}\right)^2\frac{1}{k^4}\left|\mu_r(\epsilon_r\mu_r + \bar{\beta}^2)|\nabla_t\phi|^2\right.\right.$$

$$\left.\left. + \epsilon_r\bar{\beta}^2(\epsilon_r\mu_r + \bar{\beta}^2)|\nabla_t\psi|^2 + 4\epsilon_r\mu_r\bar{\beta}^2\hat{z}\cdot(\nabla_t\psi\times\nabla_t\phi)\right|\right\} \tag{1.14}$$

$$2\frac{\beta}{\omega}(\vec{e}\times\vec{h})\cdot\hat{z} = -\mu_0\left(\frac{\omega}{c}\right)^2\frac{1}{k^4}\left|2\bar{\beta}^2\mu_r|\nabla_t\phi|^2 + 2\bar{\beta}^4\epsilon_r|\nabla_t\psi|^2\right.$$

$$\left. + 2\bar{\beta}^2(\bar{\beta}^2 + \epsilon_r\mu_r)\hat{z}\,(\nabla_t\psi\times\nabla_t\phi)\right| \tag{1.15}$$

$$\frac{j}{\omega}(\vec{e}\times\vec{h})\cdot\hat{n} = -\mu_0\frac{1}{k^2}\left\{\left|\mu_r(\phi\nabla_t\phi) + \bar{\beta}^2(\psi\nabla_t\psi)\right|\cdot\hat{n}\right.$$

$$-\beta^2 \left| \hat{z} \times (\psi \nabla_t \phi - \phi \nabla_t \psi) \right| \cdot \hat{n} \Bigg| \tag{1.16}$$

So the functional (1.7) finally has the form

$$k_0^2 \int_S \Big| \mu_r \phi^2 + \beta^2 \psi^2) ds - \int_S \tau \mu_r |\nabla_t \phi|^2 ds - \int_S \tau \epsilon_r \beta^2 |\nabla_t \psi|^2 ds$$

$$-2 \int_S \beta^2 \tau \hat{z} \cdot (\nabla_t \psi \times \nabla_t \phi) ds - \frac{j}{\omega \mu_0 (\epsilon_r \mu_r - \beta^2)} \oint_l (\vec{e} \times \vec{h}) \cdot \hat{n} dl = 0 \tag{1.17}$$

where

$$\tau = (1 - \beta^2)/(\epsilon_r \mu_r - \beta^2)$$

$$k_0^2 = \left| \frac{\omega}{c} \right|^2 \left| 1 - \beta^2 \right| \tag{1.18}$$

If the last term is omitted from the functional the natural boundary conditions of the following type are imposed on $\vec{e}$ and $\vec{h}$:

1. Tangential electric field $\vec{e}_{tang}$ is equal to zero on the surface of the perfect electric conductor (PEC).

2. Tangential magnetic field $\vec{h}_{tang}$ is equal to zero on the surface of a perfect magnetic conductor (PMC).

2. Characteristic Impedance and Dielectric and Conductor Losses

For the dominant quasi-TEM mode the characteristic impedance of a single line is calculated using the so-called power-current definition [21]-[24]

$$Z_c = \frac{P}{II^*} \tag{2.1}$$

where P is the average power propagating along the line

$$P = \mathrm{Re}\left\{ \int_S \left(\vec{E} \times \vec{H}^* \right) d\vec{s} \right\} = \int_S \mathrm{Re}\left\{ \left(\vec{e} \times \vec{h}^* \right) \cdot \hat{z} \right\} ds \tag{2.2}$$

and I is the current induced on the strip

$$I = \int_{\Gamma_s} (\hat{n} \times \vec{h}_t)\, d\vec{l} \tag{2.3}$$

Γ_S is the contour of the strip and $\hat{n}$ unit normal on the surface of the strip.

Attenuation constants due to dielectric and conductor dissipation are calculated using a perturbational approach. We use

$$\alpha_D = \frac{P_D}{2P} \quad , \qquad \alpha_C = \frac{P_C}{2P} \tag{2.4}$$

where P_D is the power dissipated in the dielectric

$$P_D = \int_{S_d} \omega \epsilon \tan\delta \; |\vec{e}\,|^2 ds \, , \tag{2.5}$$

$\tan\delta$ is the loss tangent and S_d area of the cross-section covered by dielectric and $\vec{e}$ is the field distribution for the lossless case.

P_C is the power dissipated in the conductors

$$P_C = \int_{\Gamma_c} R_S \left| h_z^2 + |\hat{n} \times \vec{h}_t|^2 \right| dl \tag{2.6}$$

where $R_S = \sqrt{\frac{\omega\mu}{2\sigma_c}}$ is the surface resistance of the conductors and Γ_C is the boundary of all conductors and h_z , $\vec{h}_t$ are field distributions for the lossless case.

Formulas (2.1-2.6) can be expressed in terms of the field functions ϕ and ψ

$$P = \sqrt{\frac{\mu_0}{\epsilon_0}}\, \beta \left| \frac{\omega}{c} \right|^2 \frac{1}{k^4} \left| \mu_r \int_S |\nabla_t \phi|^2 ds + \epsilon_r \beta^2 \int_S |\nabla_t \psi|^2 ds \right.$$

$$+ \left| \beta^2 + \epsilon_r \mu_r \right| \int_S \hat{z} \cdot \left(\nabla_t \psi \times \nabla_t \phi \right) ds \Bigg| \tag{2.7}$$

$$I = -j \beta \frac{\omega}{c} \frac{1}{k^2} \oint_{\Gamma_s} \left\{ \hat{n} \times \left[\nabla_t \phi + \epsilon_r (\hat{z} \times \nabla_t \psi) \right] \right\} dl \tag{2.8}$$

$$P_{JD} = \sqrt{\frac{\mu_0}{\epsilon_0}} \epsilon_r \tan \delta \frac{\omega}{c} \left\{ \beta^2 \int_S \psi^2 ds + \left(\frac{\omega}{c} \right)^2 \frac{1}{k^4} \left| \mu_r^2 \int_S |\nabla_t \phi|^2 ds \right. \right.$$

$$\left. \left. + \beta^4 \int_S |\nabla_t \psi|^2 ds + 2\mu_r \beta^2 \int_S \hat{z} \cdot (\nabla_t \psi \times \nabla_t \phi) ds \right| \right\} \tag{2.9}$$

$$P_{JC} = \sqrt{\frac{\mu_0}{\epsilon_0}} \sqrt{\frac{\mu_r}{2\sigma_c}} \left[\frac{\epsilon_0}{\mu_0} \right]^{1/2} \sqrt{\frac{\omega}{c}}$$

$$\oint_{\Gamma_c} \left\{ \phi^2 + \left| \hat{n} \times [\nabla_t \phi + \epsilon_r (\hat{z} \times \nabla_t \psi) \right|^2 \right\} dl \tag{2.10}$$

3. Quasi-Static Capacitance

For the quasi-TEM mode, the capacitance can be defined as

$$C = \frac{2W_E}{V^2} \tag{3.1}$$

where W_E is the electrostatic energy per unit length of the line

$$W_E = \frac{1}{2} \int_S \epsilon |e_t|^2 ds \tag{3.2}$$

and V is the potential of the strip in respect to the shielding or ground plane

$$V = \oint_{\Gamma_1} \vec{e}_t \cdot \vec{dl} \tag{3.3}$$

where Γ_1 is the path from the middle of the strip toward the ground plane.

4. Finite Element Solution

According to the FEM procedure, the cross section of the line, i.e., domain S, is subdivided into finite elements in an arbitrary manner provided that all the dielectric interfaces coincide with the element sides. Although a variety of different elements can be chosen, the triangular first- or higher-order [26] elements are adopted in this study. It has been shown [20] that the accuracy and efficiency of computation can be substantially enhanced via the use of the high-order elements as compared to the case where only the first-order elements are employed, if the same number of nodes is used. On the other hand, the use of a large number of simple elements is clearly advantageous where a complicated boundary shape needs to be modeled.

For ordinary triangular elements the area coordinates (Fig. 2) are defined as follows:

$$\xi_i = \frac{\Delta_i}{\Delta_e} = \frac{1}{2\Delta_e}(p_i + q_i x + r_i y) \quad , \quad i = 1, 2, 3 \tag{4.1}$$

$$p_i = \begin{vmatrix} x_{i+1} & y_{i+1} \\ x_{i+2} & y_{i+2} \end{vmatrix}, \quad q_i = y_{i+2} - y_{i+1} \quad r_i = -(x_{i+2} - x_{i+1}) \tag{4.2}$$

where Δ_e is the triangle area. Coordinate lines ξ_i = const. are shown in Fig. 3.

For the high-order elements the nodes are chosen as a set of regularly spaced points (Fig. 4). For the element of order M the number of nodes is

$$MV = (M \cdot (M+1))/2 \tag{4.3}$$

which is equal to the number of terms in a complete polynomial in x,y of order M.

Within each triangle unknown functions ϕ and ψ are expanded in terms of trial functions, α_i and the nodal potentials, Φ_i, Ψ_i, $i = 1, \ldots, MV$, where MV is the number of nodes per element, as follows:

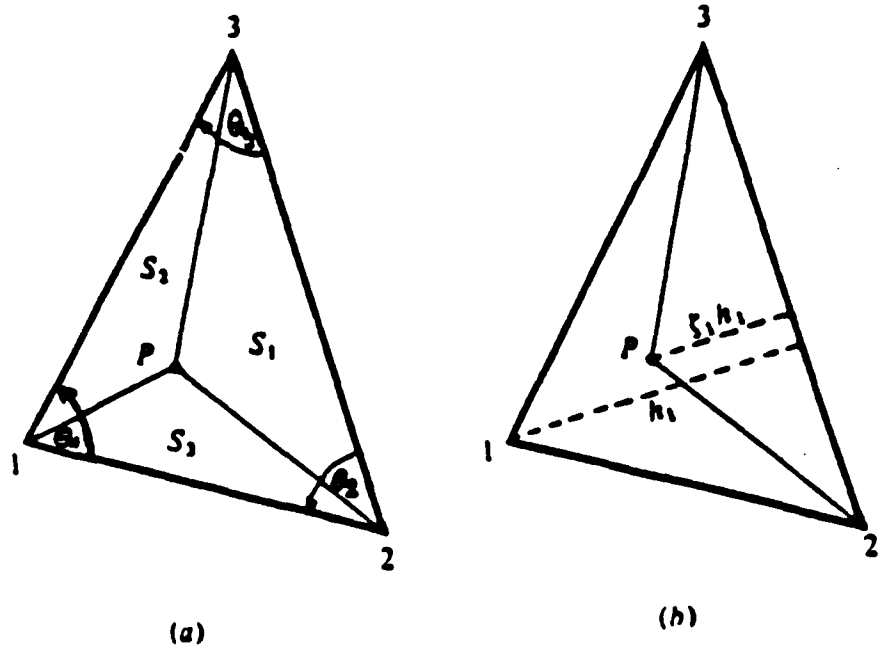

Figure 2. (a) Any interior point P defines a splitting of the triangle into subtriangles. (b) Area coordinates measure relative distance towards each vertex from the opposite side.

ξ - area coordinates

$$\xi_i = \frac{S_i}{S}, \; i = 1, 2, 3 \qquad S = S_1 + S_2 + S_3$$

$$\sum_{i=1}^{3} \xi_i = 1$$

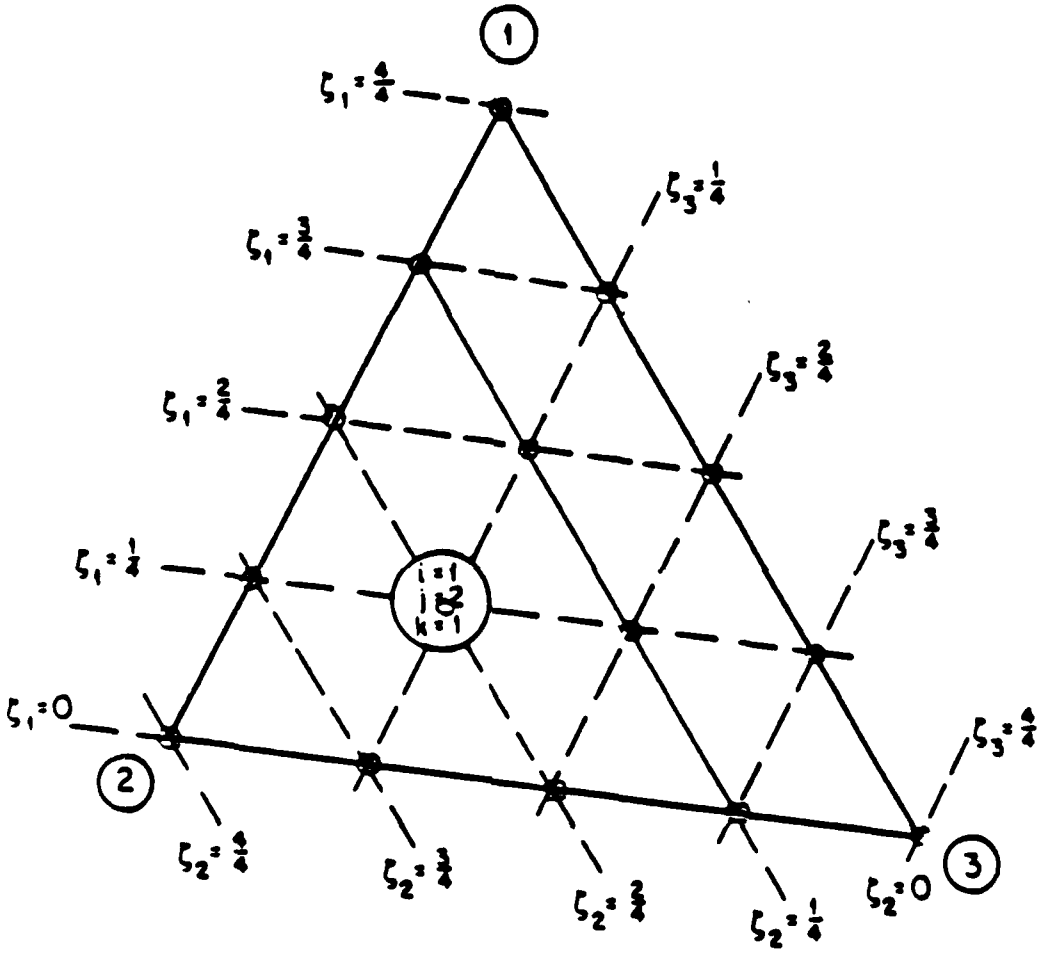

Figure 3. Lines ξ_i = constant, i = 1, 2, 3.

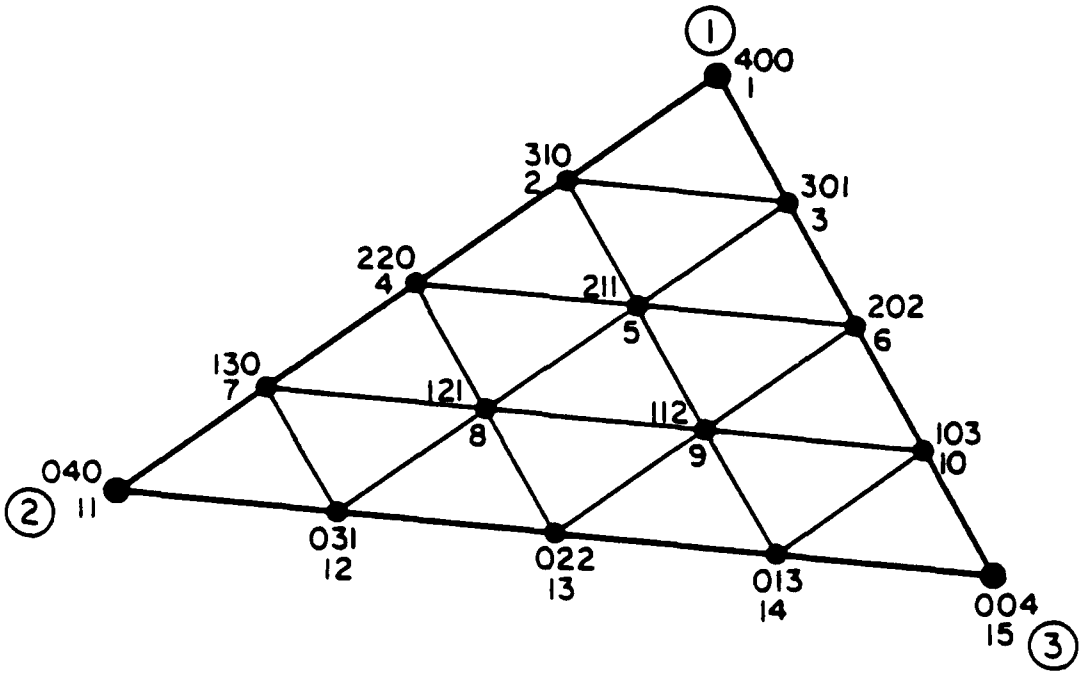

Figure 4. Point placement in a triangle for M = 4, showing the triple and single index numbering schemes as well as the numbering of triangle vertices.

$$\phi = \sum_{l=1}^{MV} \Phi_l \, \alpha_l(x,y) \;, \quad \psi = \sum_{l=1}^{MV} \Psi_l \, \alpha_l(x,y) \tag{4.4}$$

For an ordinary element of order M, the functions α_l are complete polynominals in x,y of order M and satisfy the following conditions

$$\alpha_l = 1 \quad \text{for } x = x_l, \; y = y_l \; (node \; l)$$

$$\alpha_l = 0 \quad \text{for } x = y_j, \; y = y_j, \; j \neq l \tag{4.5}$$

In accordance with the triple index ordering shown in Fig. 4, trial functions can be expressed in the following form

$$\alpha_{kmn}(\xi_1, \xi_2, \xi_3) = P_k(\xi_1) \, P_m(\xi_2) \, P_n(\xi_3) \tag{4.6}$$

where

$$P_k(\xi_i) = \prod_{j=1}^{k} \left\lfloor \frac{M \xi_i - j + 1}{j} \right\rfloor \;, k \geq 1$$

$$= 1 \quad , \qquad k = 0 \tag{4.7}$$

$$P_k \left\lfloor \frac{p}{M} \right\rfloor = 0 \;, \quad k > p$$

$$= 1 \quad , \qquad k = p$$

After introducing the expansion (4.4) the field components become

$$h_z = \phi = \sum_{l=1}^{MV} \Phi_l \, \alpha_l \tag{4.8a}$$

$$e_z = \sqrt{\frac{\mu_o}{\epsilon_o}} \, \beta \sum_{l=1}^{MV} \Psi_l \, \alpha_l \tag{4.8b}$$

$$e_x = -j \sqrt{\frac{\mu_o}{\epsilon_o}} \frac{\omega}{c} \frac{1}{k^2} \frac{1}{2\Delta_e} \sum_{l=1}^{MV} \sum_{i=1}^{3} \left| \mu_r \Phi_l r_i \frac{\partial \alpha_l}{\partial \xi_i} + \bar{\beta}^2 \Psi_l q_i \frac{\partial \alpha_l}{\partial \xi_i} \right| \tag{4.8c}$$

$$e_y = -j \sqrt{\frac{\mu_o}{\epsilon_o}} \frac{\omega}{c} \frac{1}{k^2} \frac{1}{2\Delta_e} \sum_{l=1}^{MV} \sum_{i=1}^{3} \left| -\mu_r \Phi_l q_i \frac{\partial \alpha_l}{\partial \xi_i} + \bar{\beta}^2 \Psi_l r_i \frac{\partial \alpha_l}{\partial \xi_i} \right| \tag{4.8d}$$

$$h_x = -j \bar{\beta} \frac{\omega}{c} \frac{1}{k^2} \frac{1}{2\Delta_e} \sum_{l=1}^{MV} \sum_{i=1}^{3} \left| \Phi_l q_i \frac{\partial \alpha_l}{\partial \xi_i} - \epsilon_r \Psi_l r_i \frac{\partial \alpha_l}{\partial \xi_i} \right| \tag{4.8e}$$

$$h_y = -j \bar{\beta} \frac{\omega}{c} \frac{1}{k^2} \frac{1}{2\Delta_e} \sum_{l=1}^{MV} \sum_{i=1}^{3} \left| \Phi_l r_i \frac{\partial \alpha_l}{\partial \xi_i} + \epsilon_r \Psi_l q_i \frac{\partial \alpha_l}{\partial \xi_i} \right| \tag{4.8f}$$

For the functional (1.17) we need to calculate the following terms: $\int_{\Delta_e} |\nabla_t \phi|^2 \, ds$, $\int_{\Delta_e} |\nabla_t \psi|^2 \, ds$, $\int_{\Delta_e} \hat{z} \cdot (\nabla_t \psi \times \nabla_t \phi) \, ds$, and $\int_{\Delta_e} \phi^2 \, ds$, $\int_{\Delta_e} \psi^2 \, ds$ where Δ_e is the surface of the element. After some manipulation they can be expressed in the form

$$\int_{\Delta_e} |\nabla_t \phi|^2 \, ds = \sum_{i=1}^{MV} \sum_{j=1}^{MV} \Phi_i \Phi_j S_{ij} \tag{4.9}$$

$$\int_{\Delta_e} |\nabla_t \phi|^2 \, ds = \sum_{i=1}^{MV} \sum_{j=1}^{MV} \Psi_i \Psi_j S_{ij} \tag{4.10}$$

$$\int_{\Delta_e} \hat{z} \cdot (\nabla_t \psi \times \nabla_t \phi) \, ds = \sum_{i=1}^{MV} \sum_{j=1}^{MV} \Psi_i \Phi_j U_{ij} \tag{4.11}$$

$$\int_{\Delta_e} \phi^2 \, ds = \sum_{i=1}^{MV} \sum_{j=1}^{MV} \Phi_i \Phi_j T_{ij} \tag{4.12}$$

$$\int_{\Delta_e} \psi^2 \, ds = \sum_{i=1}^{MV} \sum_{j=1}^{MV} \Psi_i \Psi_j T_{ij} \tag{4.13}$$

where S, T and U are the finite element matrices. The above matrices are given by

$$[S] = [Q_1] \cot \theta_1 + [Q_2] \cot \theta_2 + [Q_3] \cot \theta_3 \tag{4.14}$$

where

$$Q_i^{mn} = \frac{1}{2\Delta_e} \int_{\Delta_e} \left| \frac{\partial \alpha_m}{\partial \xi_{i+1}} - \frac{\partial \alpha_m}{\partial \xi_{i+2}} \right| \left| \frac{\partial \alpha_n}{\partial \xi_{i+1}} - \frac{\partial \alpha_n}{\partial \xi_{i+2}} \right| ds \,, \qquad \begin{matrix} m = 1, \ldots, MV \\ n = 1, \ldots, MV \end{matrix} \quad (4.15)$$

$cot\ \theta_i$, $i = 1,2,3$ are the included angles and matrices Q_i, $i = 1,2,3$ are symmetric and do not depend on triangle shape. The elements of the matrix U that takes into account coupling between TE and TM modes are

$$U^{mn} = \frac{1}{2\Delta_e} \sum_{i=1}^{3} \int_{\Delta_e} \left| \frac{\partial \alpha_m}{\partial \xi_{i+1}} \frac{\partial \alpha_n}{\partial \xi_{i+2}} - \frac{\partial \alpha_m}{\partial \xi_{i+2}} \frac{\partial \alpha_n}{\partial \xi_{i+1}} \right| ds \,, \qquad \begin{matrix} m = 1, \ldots, MV \\ n = 1, \ldots, MV \end{matrix} \quad (4.16)$$

This matrix is antisymmetric and does not depend on triangle shape.

The elements of matrix T have the form

$$T^{mn} = \int_{\Delta_e} \alpha_m \, \alpha_n \, ds = 2\Delta_e \int_0^1 \int_0^{1-\xi_2} \alpha_m \, \alpha_n \Big|_{\xi_3 = 1-\xi_1-\xi_2} d\xi_1 \, d\xi_2 \quad (4.17)$$

This matrix is also symmetric. The functional (1.17) now has the form

$$k_o^2 \left| \mu_r \, \Phi^T \, T \Phi + \beta^2 \Psi^T \, T \Psi \right| - \tau \mu_r \, \Phi^T \, S \Phi - \tau \epsilon_r \, \beta^2 \Psi^T \, S \Psi - 2\beta^2 \tau \Psi^T U \Phi = 0 \quad (4.18)$$

where Φ, Ψ are column matrices of nodal potentials and Φ^T, Ψ are their transpose values.

Unknown nodal potentials are found by differentiating the functional (4.18). The following system of FEM equations is then obtained

$$\sum_{i=1}^{MV} \left| \tau \mu_r \, S_{ij} \, \Phi_i + \beta^2 \tau U_{ij} \, \Psi_i \right| = \sum_{i=1}^{MV} k_o^2 \mu_r \, T_{ij} \, \Phi_i$$

$$j = 1,2, \cdots MV$$

$$\sum_{i=1}^{MV} \left| \tau \epsilon_r \beta^2 S_{ij} \, \Psi_i + \beta^2 \tau U_{ji} \, \Phi_i \right| = \sum_{i=1}^{MV} k_o^2 \beta^2 T_{ij} \, \Psi_i \quad (4.19)$$

which can be rewritten in the form

$$A \cdot X = k_o^2 \, B \cdot X \tag{4.20}$$

where X is the column matrix of all nodal potentials (Ψ_t, Φ_t), $X = \begin{Bmatrix} \Psi_t \\ \Phi_t \end{Bmatrix}$. Equation (4.20) is an ordinary matrix eigenvalue problem whose eigenvalue and eigenvectors are k_o^2 and $\begin{Bmatrix} \Psi_t \\ \Phi_t \end{Bmatrix}$, respectively. The normalized frequency $\frac{\omega}{c}$ is related to k_o^2 in the following way

$$\left| \frac{\omega}{c} \right|^2 = \frac{k_o^2}{1-\bar{\beta}^2} \tag{4.21}$$

We can use the FE-matrices to express the other quantities of interest for each element.

1. Power propagating along the line:

$$P_e = \bar{\beta} \sqrt{\frac{\mu_o}{\epsilon_o}} \left| \frac{\omega}{c} \right|^2 \frac{1}{k^4} \left| \mu_r \Phi^T S \Phi + \epsilon_r \bar{\beta}^2 \Psi^T S \Psi + \left(\bar{\beta}^2 + \mu_r \epsilon_r \right) \Psi^T U \Phi \right| \tag{4.22}$$

2. Power dissipated in dielectrics

$$P_{De} = \sqrt{\frac{\mu_o}{\epsilon_o}} \frac{\omega}{c} \epsilon_r \tan\delta \left| \bar{\beta}^2 \Psi^T T \Psi \right.$$

$$+ \left| \frac{\omega}{c} \right|^2 \frac{1}{k^4} \left| \mu_r^2 \Phi^T S \Phi + \bar{\beta}^2 \Psi^T S \Psi \right.$$

$$\left. \left. + 2\mu_r \bar{\beta}^2 \Psi^T U \Phi \right| \right| \tag{4.23}$$

3. Electrostatic energy per unit length

$$W_{Ee} = \mu_o \epsilon_r \left| \frac{\omega}{c} \right|^2 \frac{1}{k^4} \left| \mu_r^2 \Phi^T S \Phi + \bar{\beta}^2 \Psi^T S \Psi + 2\mu_r \bar{\beta}^2 \Psi^T U \Phi \right| \tag{4.24}$$

4. Current induced in side 1-2 of the triangle

$$I_{1-2} = -j\,\beta\,\frac{\omega}{c}\,\frac{1}{k^2}\left|\Phi^T QI_1 + \epsilon_r\left|\Psi^T QI_2 \cot\theta_1 + \Psi^T QI_3 \cot\theta_2\right|\right| \tag{4.25}$$

where QI_1, QI_2, QI_3 are the column matrices of dimension MV and have the following form

$$QI_i^l = \int_0^1 \left|\frac{\partial\alpha_l}{\partial\xi_i} - \frac{\partial\alpha_l}{\partial\xi_{i+1}}\right| \Bigg|_{\xi_1=1-\xi_2,\ \xi_3=0} d\xi_2 \tag{4.26}$$

5. Voltage induced in side 1-2 of the triangle

$$V_{1-2} = j\sqrt{\frac{\mu_o}{\epsilon_o}}\,\frac{\omega}{c}\,\frac{1}{k^2}\left|-\beta^2\,\Psi^T QI_1 - \mu_r\,\Phi^T QI_2 \cot\theta_1 + \mu_r\,\Phi^T QI_3 \cot\theta_2\right| \tag{4.27}$$

6. Conductor losses in side 1-2 of the triangle

$$P_{C_{1-2}} = \sqrt{\frac{\mu_r}{2\sigma}\left|\frac{\mu_o}{\epsilon_o}\right|^{1/2}}\sqrt{\frac{\omega}{c}}\left|\ell_{12}\Phi^T P_0\,\Phi + \beta^2\left|\frac{\omega}{c}\right|^2\frac{1}{k^4}\,\frac{1}{l_{12}}\left|\Phi^T P_1\Phi\right|\right.$$

$$+ 2\epsilon_r\,\Phi^T P_2\Psi\cot\theta_1 + 2\epsilon_r\,\Phi^T P_3\Psi\cot\theta_2 + \epsilon_r^2\Psi^T P_4\Psi\cot^2\theta_1 \tag{4.28}$$

$$\left. + \epsilon_r^2\Psi^T P_5\Psi\cot\theta_1\cot\theta_2 + \epsilon_r^2\Psi^T P_6\Psi\cot^2\theta_2\right|$$

where ℓ_{12} is the length of the side 1-2 and $P_0 - P_6$ are the FE-matrices which do not depend on the triangle shape

$$P_0^{mn} = \int_0^1 \alpha_m\,\alpha_n \Big|_{\xi_1=1-\xi_2,\ \xi_3=0} d\xi_2 \tag{4.29a}$$

$$P_1^{mn} = \int_0^1 \left| \frac{\partial \alpha_m}{\partial \xi_1} - \frac{\partial \alpha_m}{\partial \xi_2} \right| \left| \frac{\partial \alpha_n}{\partial \xi_1} - \frac{\partial \alpha_n}{\partial \xi_2} \right| \Bigg|_{\substack{d\,\xi_2 \\ \xi_1=1-\xi_2,\ \xi_3=0}} \tag{4.29b}$$

$$P_2^{mn} = -\int_0^1 \left| \frac{\partial \alpha_m}{\partial \xi_1} - \frac{\partial \alpha_m}{\partial \xi_2} \right| \left| \frac{\partial \alpha_n}{\partial \xi_2} - \frac{\partial \alpha_n}{\partial \xi_3} \right| \Bigg|_{\substack{d\,\xi_2 \\ \xi_1=1-\xi_2,\ \xi_3=0}} \tag{4.29c}$$

$$P_3^{mn} = \int_0^1 \left| \frac{\partial \alpha_m}{\partial \xi_1} - \frac{\partial \alpha_m}{\partial \xi_2} \right| \left| \frac{\partial \alpha_n}{\partial \xi_3} - \frac{\partial \alpha_n}{\partial \xi_1} \right| \Bigg|_{\substack{d\,\xi_2 \\ \xi_1=1-\xi_2,\ \xi_3=0}} \tag{4.29d}$$

$$P_4^{mn} = \int_0^1 \left| \frac{\partial \alpha_m}{\partial \xi_2} - \frac{\partial \alpha_m}{\partial \xi_3} \right| \left| \frac{\partial \alpha_n}{\partial \xi_2} - \frac{\partial \alpha_n}{\partial \xi_3} \right| \Bigg|_{\substack{d\,\xi_2 \\ \xi_1=1-\xi_2,\ \xi_3=0}} \tag{4.29e}$$

$$P_5^{mn} = -\int_0^1 \left| \left| \frac{\partial \alpha_m}{\partial \xi_2} - \frac{\partial \alpha_m}{\partial \xi_3} \right| \left| \frac{\partial \alpha_n}{\partial \xi_3} - \frac{\partial \alpha_n}{\partial \xi_1} \right| + \left| \frac{\partial \alpha_m}{\partial \xi_3} - \frac{\partial \alpha_m}{\partial \xi_1} \right| \left| \frac{\partial \alpha_n}{\partial \xi_2} - \frac{\partial \alpha_n}{\partial \xi_3} \right| \right| \Bigg|_{\substack{d\,\xi_2 \\ \xi_1=1-\xi_2,\ \xi_3=0}} \tag{4.29f}$$

$$P_6^{mn} = \int_0^1 \left| \frac{\partial \alpha_m}{\partial \xi_3} - \frac{\partial \alpha_m}{\partial \xi_1} \right| \left| \frac{\partial \alpha_n}{\partial \xi_3} - \frac{\partial \alpha_n}{\partial \xi_1} \right| \Bigg|_{\substack{d\,\xi_2 \\ \xi_1=1-\xi_2,\ \xi_3=0}} \tag{4.29g}$$

5. Special FEM Elements

In order to enhance the accuracy and efficiency of the presented FEM procedure special elements as singular and infinite elements have been used.

When there are field singularities caused by edges in the cross section of the line, a very fine mesh of first- or high-order elements is required to obtain an accurate solution. However, in order to improve accuracy and reduce the number of necessary nodes, singular elements [27], [28] are used in this study. A singular element with associated triangular polar coordinate system (ρ, σ) is shown in Figure 5.

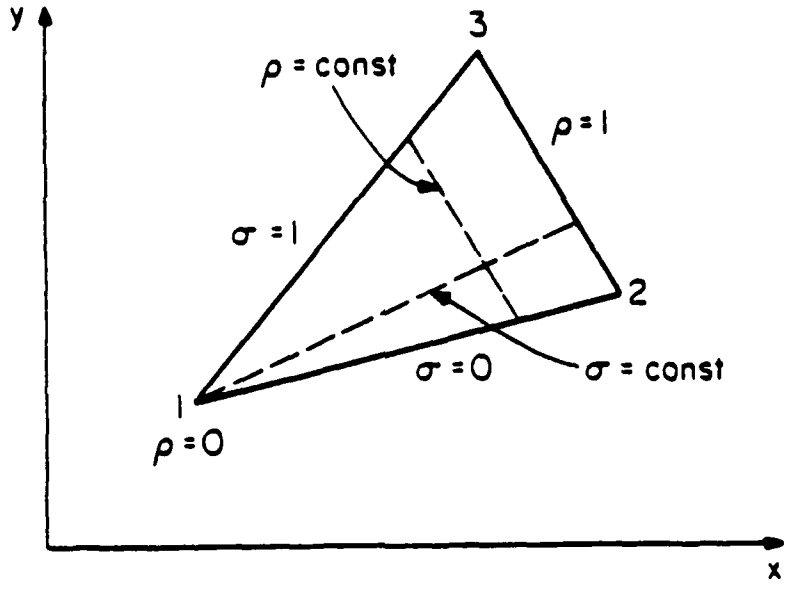

Figure 5. Singular element.

The global Cartesian coordinates are then

$$x = x_1 + \rho\,[(x_2 - x_1) + \sigma\,(x_3 - x_2)] \tag{5.1}$$
$$y = y_1 + \rho\,[(y_2 - y_1) + \sigma\,(y_3 - y_2)]$$

The potential distribution function, ϕ or ψ, that takes into account the field singularity at the node 1 ($\rho = 0$) has the following form:

$$\phi = \sum_{i=0}^{M} R_i(\rho) \sum_{k=0}^{i} L_k^i(\sigma)\,\Phi_{ik} \tag{5.2}$$

where $R_i(\rho)$ is a polynominal of the form [28]

$$R_i(\rho) = a_{i0} + a_{i1}\rho^{\lambda} + a_{i2}\,\rho^{\lambda+1} + \cdots + a_{ii}\,\rho^{\lambda+i-1} \tag{5.3}$$

and λ is a coefficient chosen in accordance with the Meixner edge condition [29]. $L_k^i(\sigma)$ are Lagrange interpolation polynominals:

$$L_k^i(\sigma) = \frac{\sigma(\sigma - \frac{1}{i})\cdots(\sigma - \frac{k-1}{i})\,(\sigma - \frac{k+1}{i})\cdots(\sigma - 1)}{\frac{1}{i}\cdots\frac{k-1}{i}\;\;\frac{k+1}{i}\cdots 1} \tag{5.4}$$

Φ_{ijk} are nodal potentials for the nodes regularly spaced in the triangle (Fig. 6). These elements are compatible with high-order ordinary elements.

Although open-type transmission lines can be treated by the conventional finite element method with the shielding far away from the region of interest, the computation efficiency can be substantially improved if infinite elements [30] are used. Consider first the line consisting of a number of conductors arbitrarily placed between two parallel ground planes (Fig. 7a).

The entire domain can be divided into the near-field region (n.f.), which is the region of interest, and the far-field region (f.f.), which is unbounded. They have a common boundary referred to as the far-field boundary (f.f.b). The near field (n.f.) region is then divided into finite triangular elements in the usual manner, while the f.f. region is divided

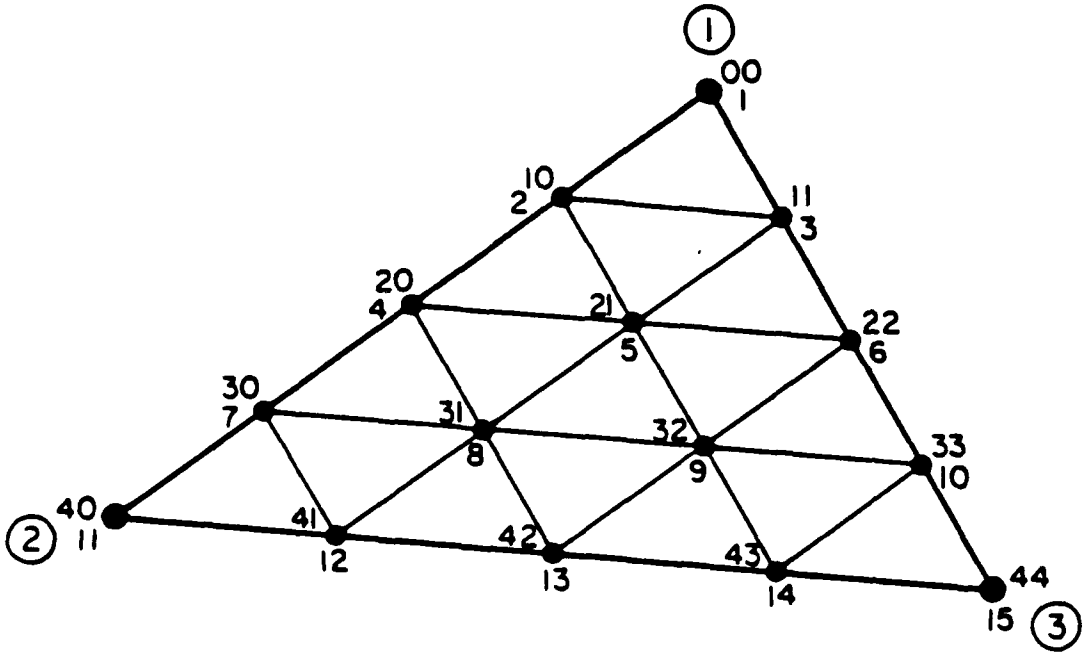

Figure 6. Point placement in a triangle for M=4, showing double and single index numbering schemes, as well as the numbering of triangle vertices.

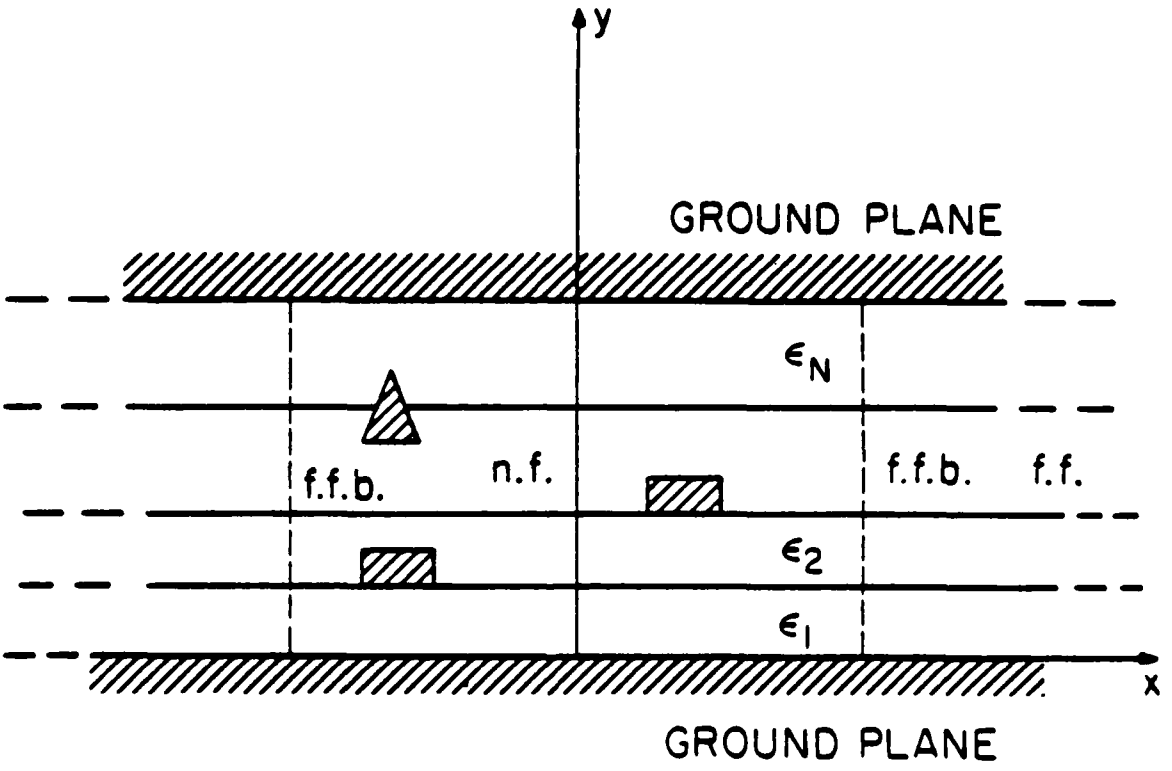

Figure 7a. Line consisting of a system of conductors placed between two ground planes.

into infinite elements. Each infinite element has one common side (lying on f.f.b) with an ordinary element and two sides parallel to the x-axis.

Consider the infinite element with nodes 1 and 2 (Fig. 7b) and introduce normalized coordinates

$$\xi = \frac{x}{x_1}, \quad \eta = \frac{y - y_1}{y_2 - y_1}, \quad x_1 < x < \infty, \quad y_1 \leqslant y \leqslant y_2 \tag{5.5}$$

Thus, in the normalized coordinates ξ, η the potential function ϕ can be written in terms of the nodal potentials as:

$$\phi = e^{-a\xi} \sum_{i=0}^{M} L_i^M(\eta)\, \Phi_i \tag{5.6}$$

where L_i^M are Lagrange interpolation polynomials and Φ_i are corresponding nodal potentials.

The next type of open region problem is a system of conductors above a ground plane. The procedure is similar to that in the previous case. The entire domain is divided into n.f. and f.f. regions (Fig. 8a). The n.f. region is divided into the usual triangular mesh and the f.f. region is divided into infinite elements of two different types, I and II. The infinite element type I is the element previously discussed. Consider now the infinite element of type II with nodes 1, 2 and radial sides intersecting at point (x_o, y_o) (Fig. 8b) and introduce triangular polar coordinates ρ, σ which are related to the global Cartesian coordinates by the relations

$$x = x_o + \rho\,[\,(x_1 - x_o) + \sigma(x_2 - x_1)\,] \tag{5.7}$$

$$y = y_o + \rho\,[\,(y_1 - y_o) + \sigma(y_2 - y_1)\,]$$

In the similar way as for the element type I the potential distribution within element type II is approximated by

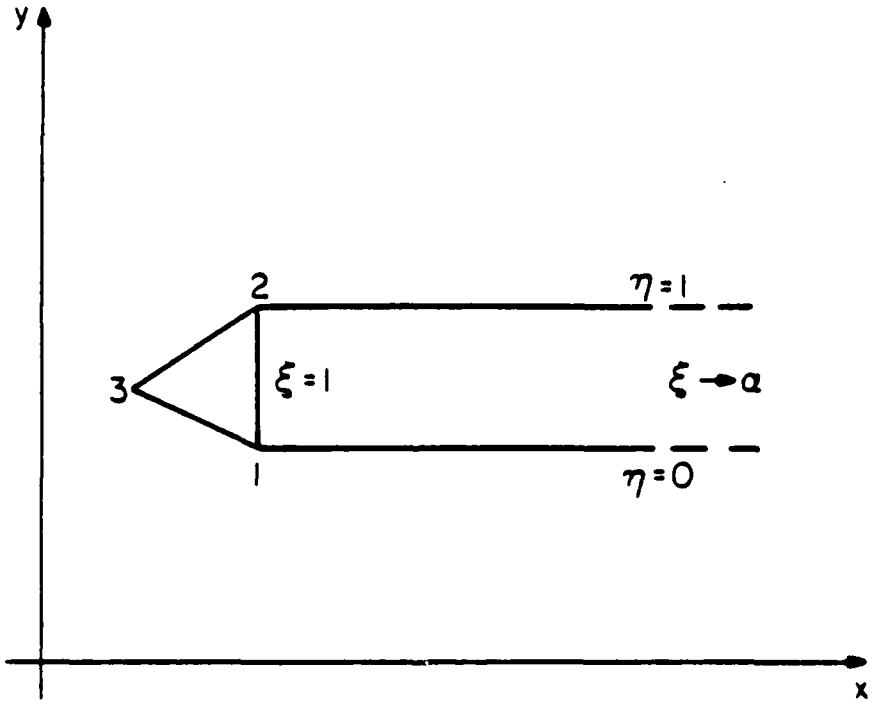

Figure 7b. Infinite element type I.

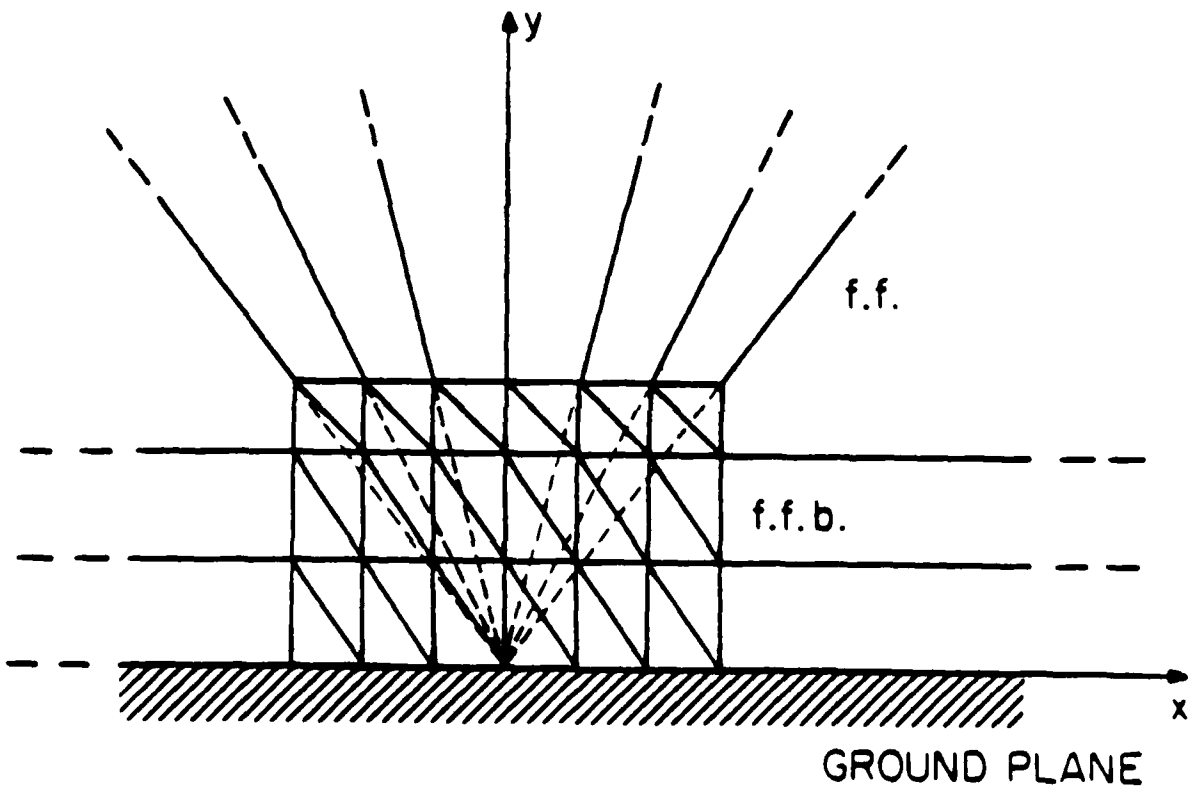

Figure 8a. Line consisting of a system of conductors placed above a ground plane.

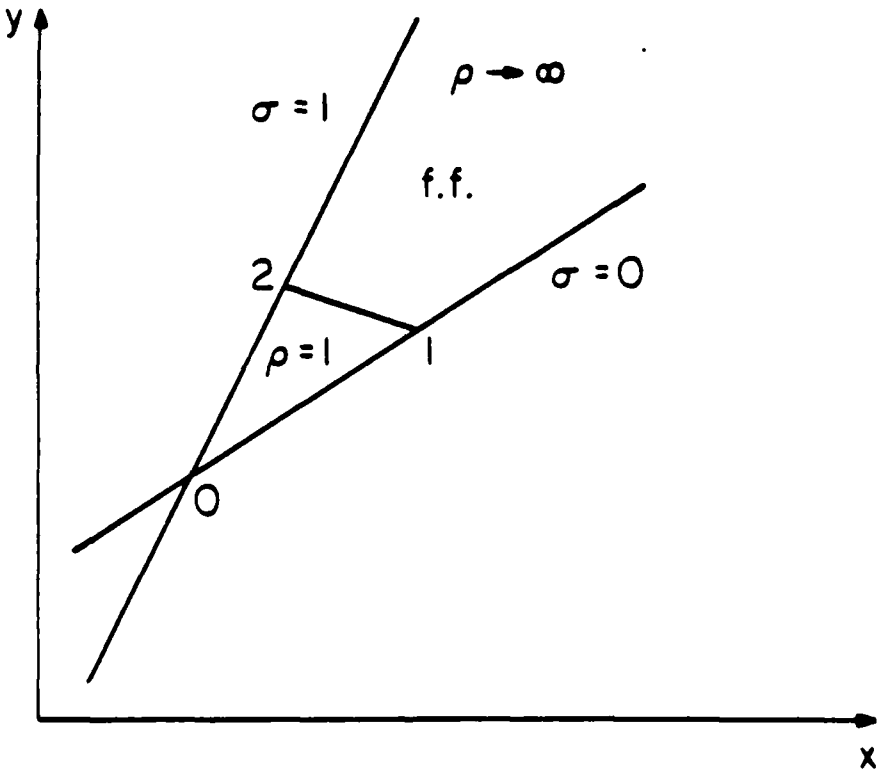

Figure 8b. Infinite element type II.

$$\phi = e^{-a\rho} \sum_{i=0}^{M} L_i^M(\sigma)\, \Phi_i \tag{5.8}$$

Both infinite elements type I and type II are compatible with high-order ordinary elements of order M.

Coefficient a is varied as well as the position of the f.f.b until the convergence of the solution is obtained.

III. NUMERICAL RESULTS

On the basis of described finite element procedures, two different computer software packages have been developed for solving the problem at hand. The first of these is employed for semiautomatic mesh generation of first- or high-order ordinary elements including singular and infinite elements if necessary. The second package solves for the dispersion characteristics and the field distributions of the propagating modes. Using the obtained field distribution for each mode it then calculates the characteristic impedance of the line and attenuation due to conductor and dielectric losses.

Different types of microstrip lines have been analyzed and some of the results are presented in this study.

In Fig. 9, the generic cross-section of the shielded microstrip line is presented. The width of the line is 2w and the thickness t. Height of the substrate is h and the height of the shielding is b. The width of the shielding is 2a.

For the special case when the permittivity of the substrate is $\epsilon_r = 4\epsilon_0$ dispersion characteristics of the first four propagating modes are presented in Fig. 10. Values of β^2 are plotted versus normalized frequency $(\omega h/c)^2$. It should be pointed out that for the thickness of the substrate h = 1mm actual frequency for $(\omega h/c)^2 = 1$ is about 50 GHz. The dominant mode is a quasi-TEM mode. Another mode which propagates from the zero frequency is the surface-wave mode. The other two modes are waveguide modes. In

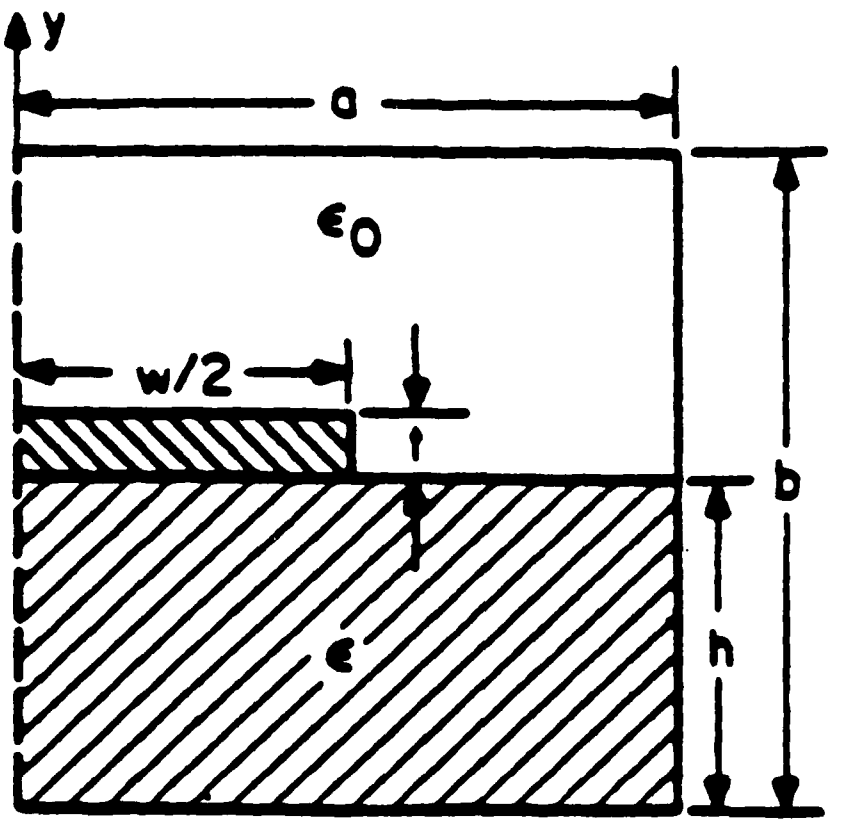

Figure 9. Generic cross-section of shielded micro-strip line.

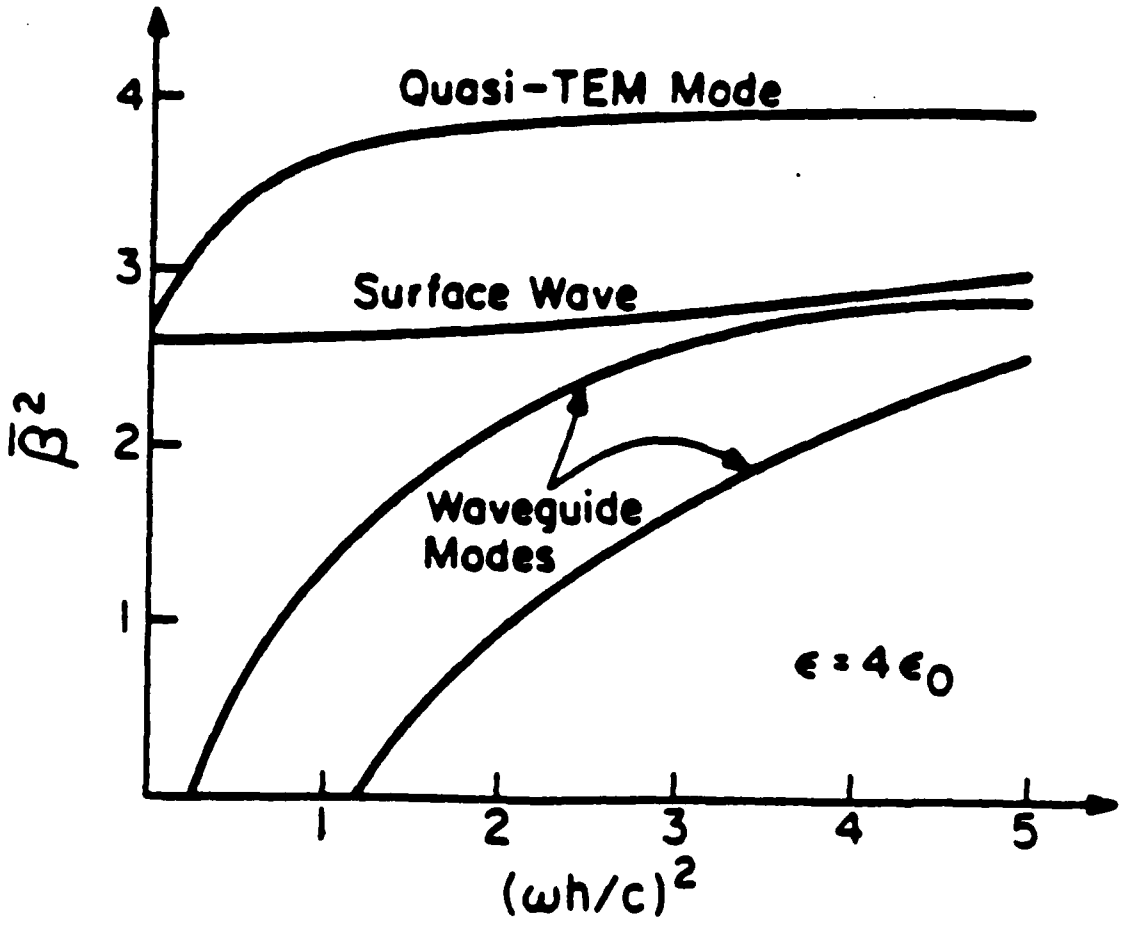

Figure 10. Plot of $\bar{\beta}^2$ vs. $(\omega h/c)^2$ for first four modes of shielded microstrip line.

Fig. 11, the results for the characteristic impedance of the dominant mode are presented up to a frequency of 40 GHz. In this case permittivity is $\epsilon = 4\epsilon_0$ and the height of the substrate h = 0.5mm.

For the same line the results for the attenuation constant due to conductor losses are presented in Fig. 12 and for the attenuation constant due to dielectric losses in Fig. 13.

Also, the coupled lines have been analyzed. The generic cross-section of one half of the line is presented in Fig. 14.

Both even- and odd-modes have been analyzed. In Fig. 15, the dispersion characteristics of the first four propagating even-modes are presented while in Fig. 16 the odd-modes are plotted.

IV. CONCLUSIONS

In this study a full-wave analysis of microwave transmission lines has been performed. The analysis is based on a hybrid-mode model which takes into account the coupling between TE- and TM modes propagating along the line. The finite-element method has been used to solve for the propagation constant (eigenvalues) and the field distribution (eigenvectors) of each mode. High-order ordinary elements as well as singular and infinite elements have been employed. Using the obtained field distribution the characteristic impedance of the dominant, quasi-TEM, mode has been calculated. Finally, a perturbational approach has been used to compute the attenuation constant due to conductor and dielectric losses.

A general computer software package has been developed for semi-automatic mesh generation and for computation of the propagation and attenuation constants and the characteristic impedance. Some of the results for isolated and coupled microwave transmission lines are presented and a good agreement with available data has been found.

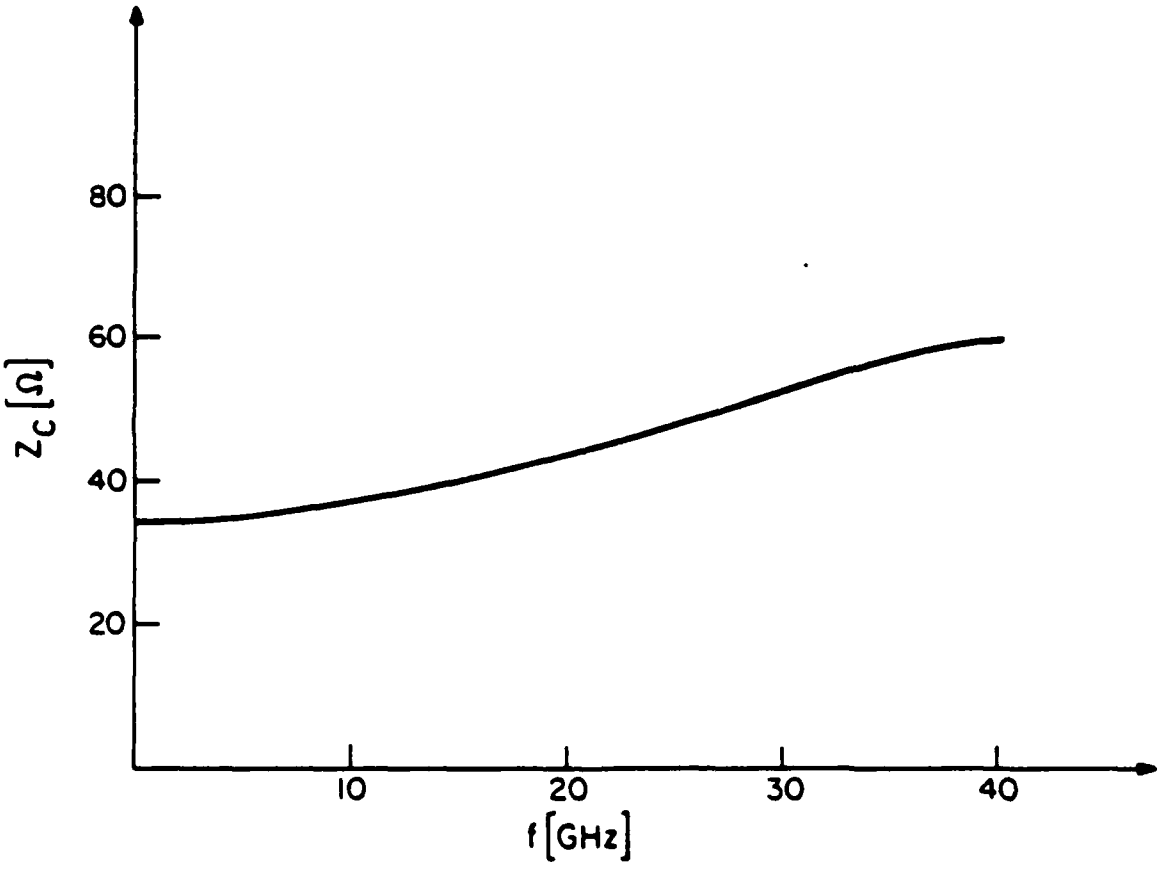

Figure 11. Characteristic impedance of shielded micro-strip line
h = 0.5 mm, ϵ_r = 4

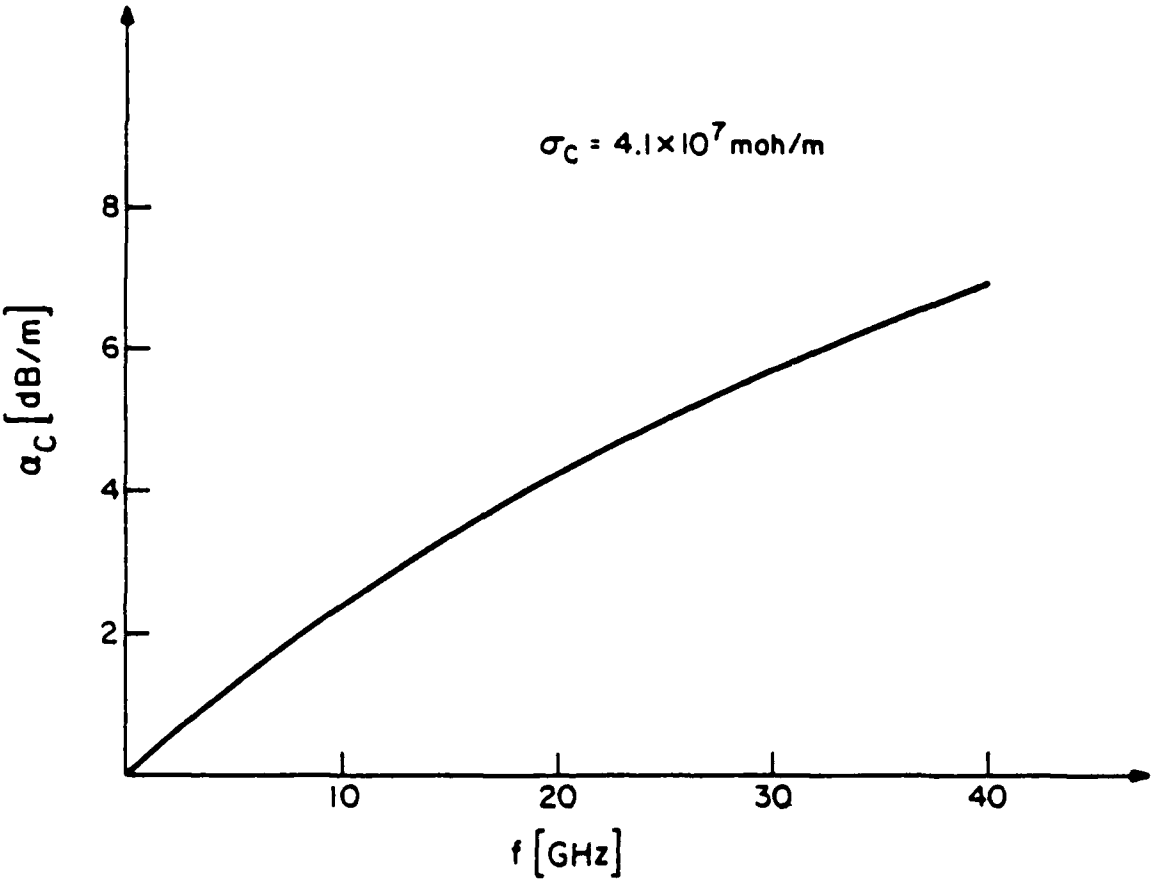

Figure 12. Conductor losses of shielded micro-strip line
h = 0.5 mm, $\epsilon_r = 4$

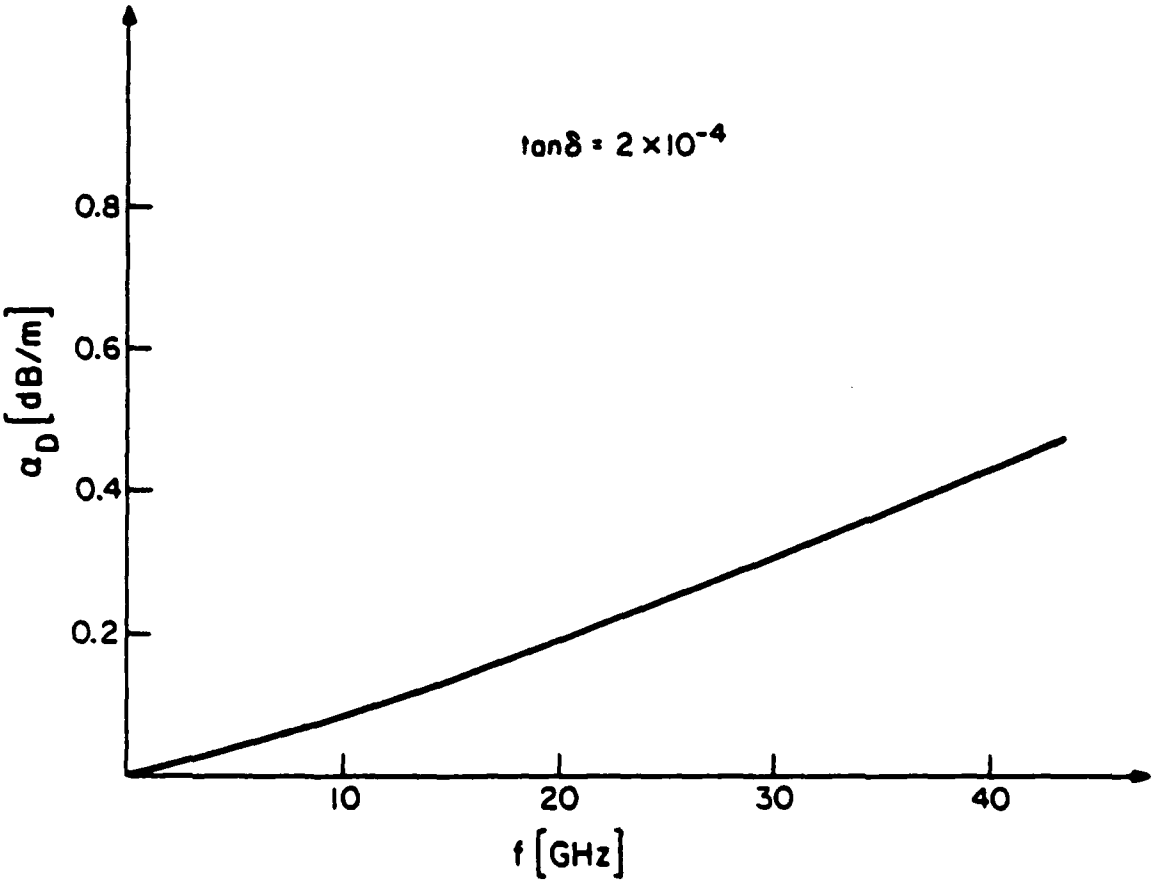

Figure 13. Dielectric losses for shielded micro-strip line
h = 0.5 mm, $\epsilon_r = 4$

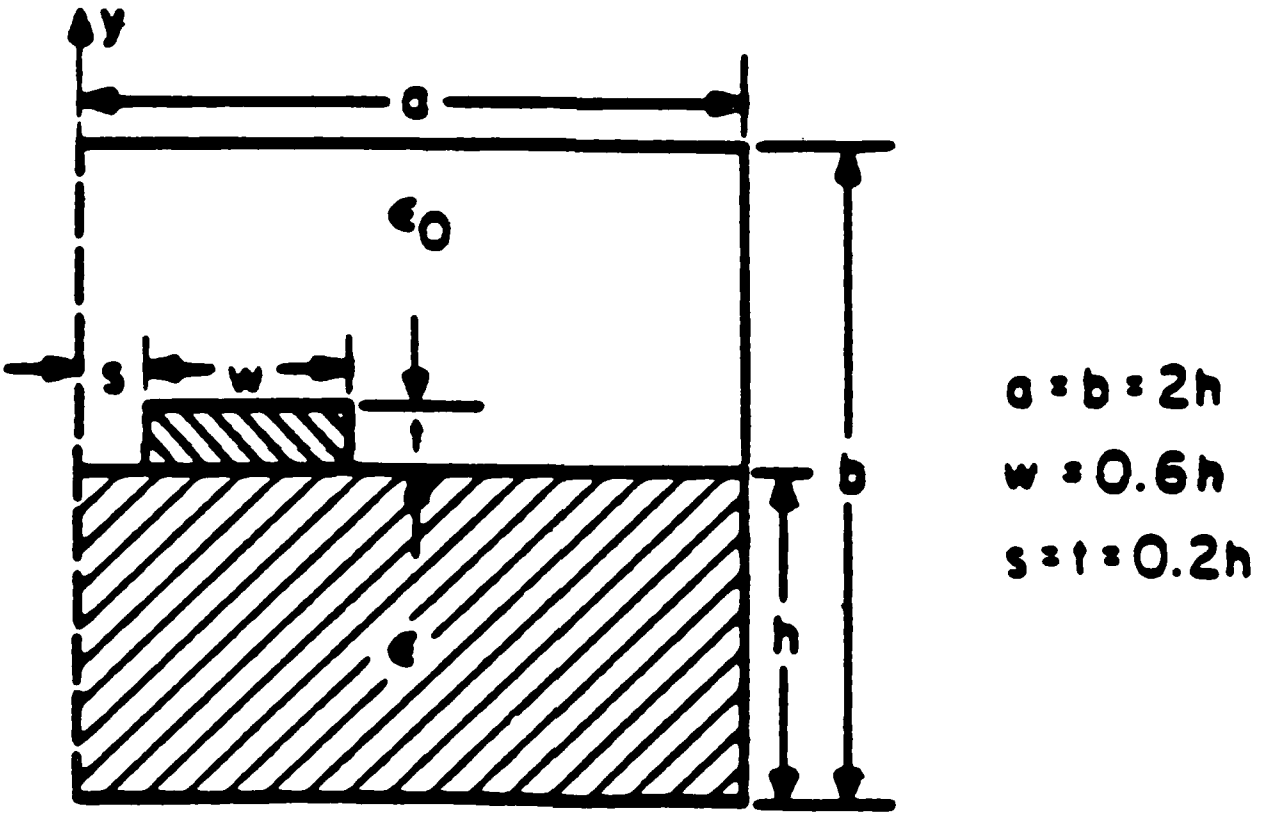

Figure 14. Generic cross section of one half of shielded coupled microstrip line.

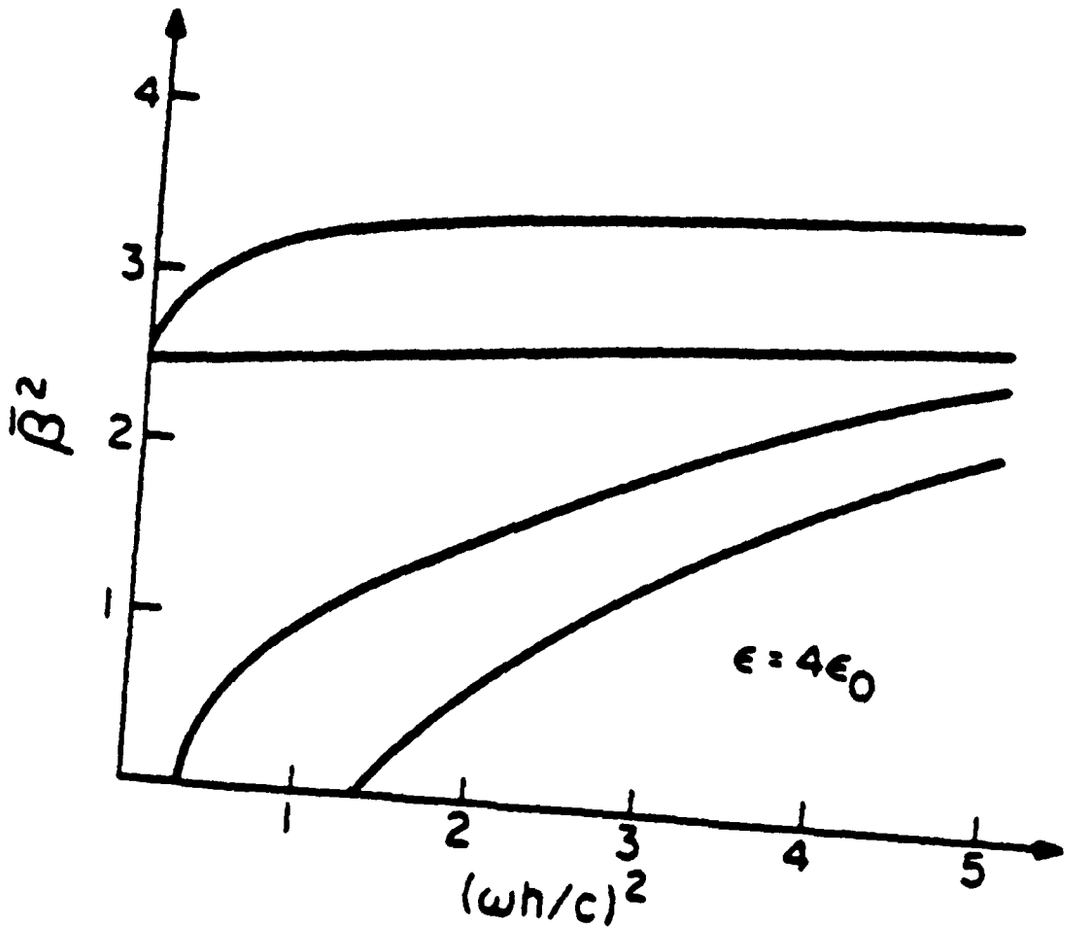

Figure 15. Plot of $\bar{\beta}^2$ vs. $(\omega h/c)^2$ for first four even modes of shielded coupled micro-strip line.

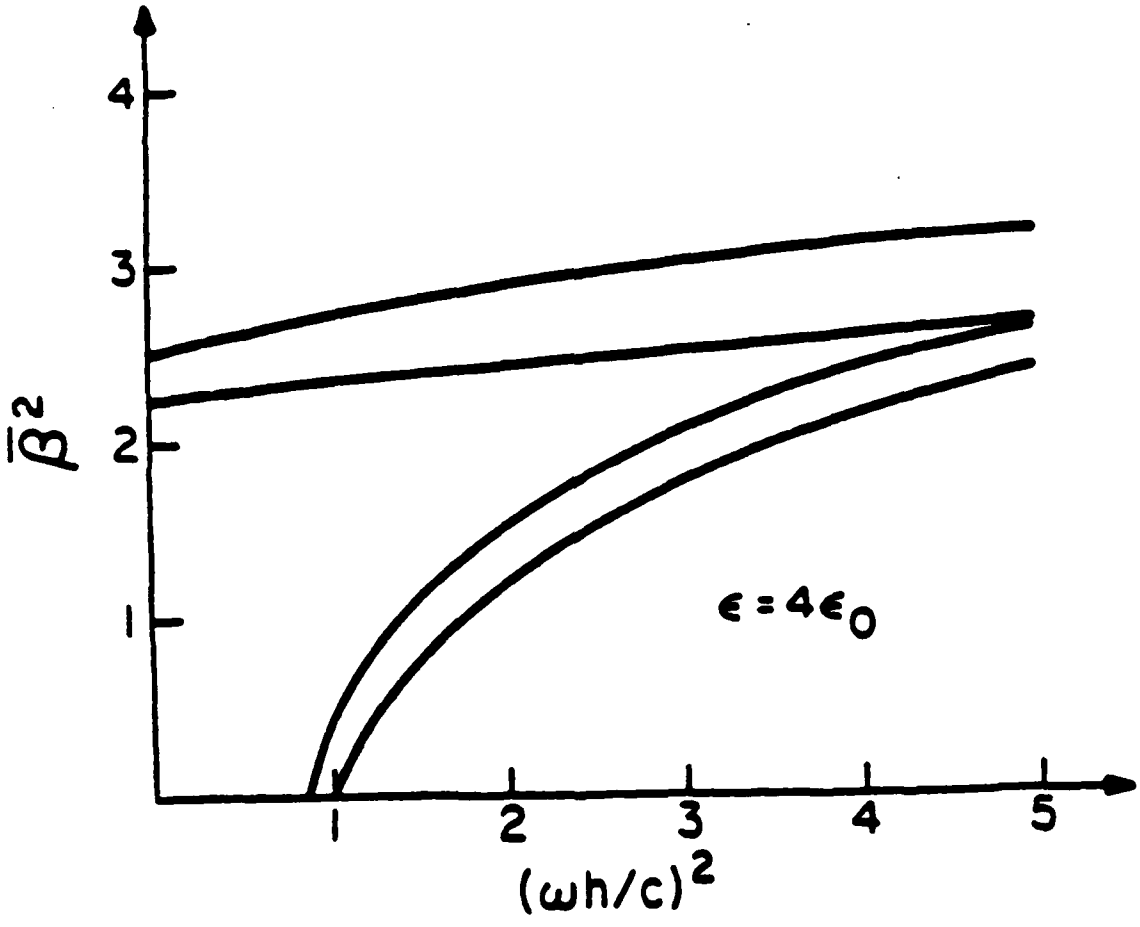

Figure 16. Plot of $\bar{\beta}^2$ vs. $(\omega h/c)^2$ for first four odd modes of shielded coupled micro-strip line.

REFERENCES

[1] P. Silvester, "TEM wave properties of microstrip transmission lines," *Proc. Inst. Elec. Eng.*, vol. 115, pp. 43-48, Jan. 1968.

[2] T. G. Bryant and T. A. Weiss, "Parameters of microstrip transmission lines and of coupled pairs of microstrip lines," *IEEE Trans. Microwave Theory Tech.*, vol. MTT-16, pp. 1021-1027, Dec. 1968.

[3] E. Yamashita, K. Atsuki, "Analysis of thick-strip transmission lines," *IEEE Trans. Microwave Theory Tech.*, vol. MTT-19, pp. 120-122, Jan. 1971.

[4] R. Crampagne, M. Ahmadpanah, and T. Guirand, "A simple method for determining the Green's function for a large class of MIC lines having multilayered dielectric structures," *IEEE Trans. Microwave Theory Tech.*, vol. MTT-26, pp. 82-87, Feb. 1978.

[5] C. Wei, R. Harrington, L. Mautz and T. Sarkar, "Multiconductor lines in multilayered dielectric media," *IEEE Trans. Microwave Theory Tech.*, vol. MTT-32, pp. 439-449, April 1984.

[6] R. Mittra and C. Chan, "Iterative approaches to the solution of electromagnetic boundary value problems," *Electromagnetics*, vol. 5, no. 2-3, pp. 123-146, 1985.

[7] S. Cohn, "Characteristic impedances of broadside-coupled strip transmission lines," *IRE Trans. Microwave Theory Tech.*, vol. MTT-8, pp. 633-637, Nov. 1960.

[8] T. Chen, "Determination of the capacitance, inductance, and characteristic impedance of rectangular lines," *IRE Trans. Microwave Theory Tech.*, vol. MTT-8, pp. 510-519, Sept. 1960.

[9] H. A. Wheeler, "Transmission-line properties of parallel strips separated by a dielectric sheet," *IEEE Trans. Microwave Theory Tech.*, vol. MTT-13, pp. 172-185, Mar. 1965.

[10] E. Yamashita and R. Mittra, "Variational method for the analysis of microstrip lines," *IEEE Trans. Microwave Theory Tech.*, vol. MTT-16, pp. 251-256, Apr. 1968.

[11] S. K. Koul and B. Bhat, "Generalized analysis of microstrip-like transmission lines and coplanar strips with anisotropic substrates for MIC, electro-optic modulator, and SAW application," *IEEE Trans. Microwave Theory Tech.*, vol. MTT-31, pp. 1051-1058, Dec. 1983.

[12] R. Mittra and T. Itoh, "Charge and potential distributions in shielded striplines," *IEEE Trans. Microwave Theory Tech.*, vol. MTT-18, pp. 149-156, Mar. 1970.

[13] A. El-Sherbiny, "Exact analysis of shielded microstrip lines and bilateral fin lines," *IEEE Trans. Microwave Theory Tech.*, vol. MTT-29, pp. 669-675, July 1981.

[14] A. Farrar and A. T. Adams, "Computation of propagation constants for the fundamental and higher order modes in microstrip," *IEEE Trans. Microwave Theory Tech.*, vol. MTT-24, pp. 456-460, July 1976.

[15] T. Itoh and A. S. Herbert, "A generalized spectral domain analysis for coupled suspended microstriplines with tuning septums," *IEEE Trans. Microwave Theory Tech.*, vol. MTT-26, pp. 820-826, Oct. 1978.

[16] T. Itoh, "Generalized spectral domain method for multiconductor printed lines and its application to tunable suspended microstrips," *IEEE Trans. Microwave Theory Tech.*, vol. MTT-26, pp. 983-987, Dec. 1978.

[17] D. M. Syahkal and J. B. Davies, "Accurate solution of microstrip and coplanar structures for dispersion and for dielectric and conductor losses," *IEEE Trans. Microwave Theory Tech.*, vol. MTT-27, pp. 694-699, July 1979.

[18] R. F. Harrington et al., "Computation of Laplacian potentials by an equivalent source method," *Proc. Inst. Elec. Eng.*, vol. 116, no. 10, pp. 1715-20, Oct. 1969.

[19] B. E. Spielman, "Dissipation loss effects in isolated and coupled transmission lines," *IEEE Trans. Microwave Theory Tech.*, vol. MTT-25, pp. 648-655, Aug. 1977.

[20] P. Daly, "Hybrid-mode analysis of microstrip by finite-element method," *IEEE Trans. Microwave Theory Tech.*, vol. MTT-19, pp. 19-25, Jan. 1971.

[21] F. Arndt and G. V. Paul, "The reflection definition of the characteristic impedance of

microstrips," *IEEE Trans. Microwave Theory Tech.*, vol. MTT-27, pp. 724-731, Aug. 1979.

[22] R. H. Jansen, "Unified user-oriented computation of shielded, covered, and open planar microwave and millimeter-wave transmission-line characteristics," *IEEE Proc. Pt. H., Microwaves Opt. Acoust.*, vol. MOA-1, pp. 14-22, Jan. 1979.

[23] B. Bianco, et al., "Some considerations about the frequency dependence of uniform microstrips," *IEEE Trans. Microwave Theory Tech.*, vol. MTT-26, pp. 182-185, Mar. 1978.

[24] W. J. Getsinger, "Microstrip characteristic impedance," *IEEE Trans. Microwave Theory Tech.*, vol. MTT-27, p. 293, Aapr. 1979.

[25] R. F. Harrington, *Time Harmonic Electromagnetic Fields*. New York: McGraw Hill, 1960.

[26] P. Silvester, "High-order polynomial triangular finite elements for potential problems," *Int. J. Engrg. Sci.*, vol. 7, pp. 849-861, 1969.

[27] Z. Pantic and R. Mittra, "Quasi-TEM analysis of microwave transmission lines by the finite element method," to be published in *IEEE Trans. Microwave Theory Tech.*

[28] P. Tracey and T. Cook, "Analysis of power type singularities using finite elements," *Int. J. Num. Methods Engrg.*, vol. 11, pp. 1225-1233, 1977.

[29] J. Meixner, "The behaviour of electromagnetic fields at edges," Inst. Math. Sci. Res. Rept. EM-72, New York University, New York, NY, Dec. 1954.

[30] F. Medina and R. Taylor, "Finite element techniques for problems of unbounded domains," *Int. J. Num. Methods Engrg.*, vol. 19, pp. 1209-1226, 1983.

END

4-87

DTIC